Experimental study of the static and dynamic behavior of pre-stressed concrete subjected to shear loading

Reem Abdul-Rahman, Dominique Saletti, Pascal Forquin

Experimental study of the static and dynamic behavior of pre-stressed concrete subjected to shear loading

Reem Abdul-Rahman[1], Pascal Forquin[1], Dominique Saletti[1]

[1]Univ. Grenoble Alpes, CNRS, Grenoble INP, 3SR laboratory, 38000 Grenoble, France

Abstract: In the present work, the static and dynamic shear strength of concrete is investigated by means of Punch-Through Shear (PTS) tests. This experimental method consists in applying an axial load to the central part of the specimen which generates shear stresses in the ligament of the sample. Prior to the shearing stage, the concrete sample is subjected to a lateral confinement pressure that is applied by pre-stressing a metallic cell and then inserting the sample in-between the cell jaws so the confinement stresses are transferred to the concrete specimen during the unloading. The originality of this method lies then in the fact that the level of confinement is better controlled than the experimental protocol which can be found in the literature. A standard hydraulic press was used to conduct quasi-static experiments whereas a modified Split Hopkinson Pressure Bar device was used to perform the dynamic tests. The confinement cell is instrumented with strain gages so the confinement level applied to the ligament of the concrete specimen is measured before and during the shearing stage. The results on two sets of samples (dry and wet) shows that the shear strength is sensitive to the water content with higher values for dry samples and to the applied loading rate, with higher values of dynamic shear strength compared to static ones for both concretes.

Keywords: Punch-through shear test, Confinement, Split Hopkinson bar, Mode II fracture, Strain-rate sensitivity

1. Introduction

The behavior of concrete is a major issue since concrete is widely used in the construction of complex infrastructures such as protective structures, nuclear reactors, tunnels or dams. When subjected to dynamic loading such as earthquakes, blast loadings or soft and hard projectile impacts, compression, tensile and shear damage modes are observed [1-2]. The Punch-Through shear test configuration has been adapted by several authors in order to better understand the

behavior of concretes and other rock-like materials under mode II fracture in both quasi-static and dynamic regimes.

First attempts to create pure mode II crack in notched specimens were introduced by [3] and [4]. After subjecting notched beam specimens to concentrated forces, [4] stated that the failure of concrete is essentially due to shear fracture (mode II). Another new experimental technique to study materials under shear loading was considered by [5]. This technique was then developed by [6-8]. The specimen is a short cylindrical sample with two cylindrical coaxial notches on the top and bottom faces leaving a cylindrical ligament. Originally, these tests were done without confinement; an axial load is applied to the central part in order to produce mode II fractures inside the ligament. Montenegro *et al*. [7; 9] developed an experimental technique to apply a confinement up to 8 MPa to the sample prior to shearing of the ligament. The authors noted a significant increase of stresses and ductility and a reduction of dilatancy effect with the lateral confinement. Backers *et al.* [8] used the same technique on 6 different types of rocks in order to determine mode II fracture toughness. The authors applied a confinement up to 80 MPa on the specimens and established a bilinear relation between the confinement pressure and the fracture toughness. The mode II fracture toughness of rocks was more recently investigated [10-12]. Parallely, the split Hopkinson bar technique was used to apply high strain rates loading on shear specimens. Forquin *et al* [13-14] conducted PTS experiments under quasi-static and dynamic loading on wet and saturated samples. The authors used an instrumented confining cell to induce a pressure inside the fractured zone and radial notches were performed to remove the effect of self-confinement induced by the peripheral part of the sample. Results of experiments on dry and wet concrete samples for different strain-rates showed that dry samples exhibit higher shear strength than wet ones and both concretes showed a small sensitivity to strain-rates. Lukić and Forquin [15] used the same experimental technique to study the static and dynamic shear behavior of ultra-high performance concrete and concluded that higher radial confinement stresses under high strain rate lead to an increase of the shear strength. The split Hopkinson pressure bar technique was more recently used to study the dynamic shear failure with a similar approach applied to different materials such as rocks [16] and steel [17].

The main drawback of the previous technique employed in [14] is the use of passive confinement (based on non-pre-stressed confining cell) that results in a strong change of

confinement level during the sample shearing stage. A new experimental configuration with a so-called "active confinement" applied to the concrete specimen has been recently proposed in [18]. The technique consists in using a pre-stressed metallic cell on a parallelepiped specimen. The lateral surfaces of the specimen are subjected to a confinement, and then forces are applied on an orthogonal direction creating a shear loading in the specimen. A close-form solution was proposed to predict the level of applied confinement knowing the cell and sample stiffnesses and given the difference between the sample length and the available spacing in-between the cell jaws.

In this paper, it is proposed to extend this technique to dynamic loadings in order to study the influence of the strain-rate on the confined shear response of concrete. First, the geometry of the specimen will be presented with a brief description of the confinement method. Then, the experimental results obtained in quasi-static and dynamic tests will be presented for different confinement levels and moisture contents of concrete.

2. Experimental methodology

2.1. Tested material

The present study was done on a R30A7 ordinary concrete. This concrete contains hard siliceous aggregates with a maximum aggregates size of 8mm. It was already used in quasi-static triaxial tests [19-21], in quasi-oedometric tests [22] and in bending tests [23]. Its composition and mechanical properties are listed in Table 1. After pouring, concrete blocks are stored for 1 month in water saturated with lime. Specimens are then cut and rectified and notches are done with a saw under water lubrication to avoid heating the concrete. The defect in parallelism of two opposite faces should be less than 0.05 mm to avoid a non-homogeneous distribution of stresses during tests. This was verified thanks to a surface plate and a dial indicator set-up.

The saturated specimens were kept in water until few minutes before testing. Since the drying kinetic of a saturated sample during its preparation occurs quickly, a saturated sample loses in general 20% of the water mass in its volume after 24h of exposure to air [20]. The preparation of a concrete sample requires at least 2-3 hours, so that the majority of the saturated samples

become partially saturated samples with a saturation degree between 85% and 90% at the beginning of the test.

The dried specimens were oven-dried at 60°C during several weeks until a constant weight has been achieved. The saturation ratio of the dried concrete tested in this study is approximately 11% [20].

Table 1 Composition and mechanical properties of R30A7

Concrete mix proportions	Kg/m3
Water	169
Sand D (diameter)$_{max}$ 1.8mm	838
Aggregate D 0.5 to 8mm	1007
Cement CEM I 52.5N	263
Mechanical properties	
Average Compression strength after 28 days (MPa)	28.6
Average slump (cm)	6.9
Porosity accessible to water (%)	12
W/C ratio	0.64

2.2. Specimen geometry

To apply the confinement, parallelepipedal specimens are used as shown in Figure 1(a) and Figure 1(b). The dimensions and the position of the notches are adapted for the testing of the R30A7 ordinary concrete as previously discussed in [18]. One can notice that the inner surface of the bottom notches coincides with the outer surface of the upper notches to make two straight shear fracture surfaces 40 mm apart (Figure 1(b)). The surfaces related to the application of the lateral confinement (Confining Pressure) and the shear loading (Axial Force) are depicted on Figure 1(c).

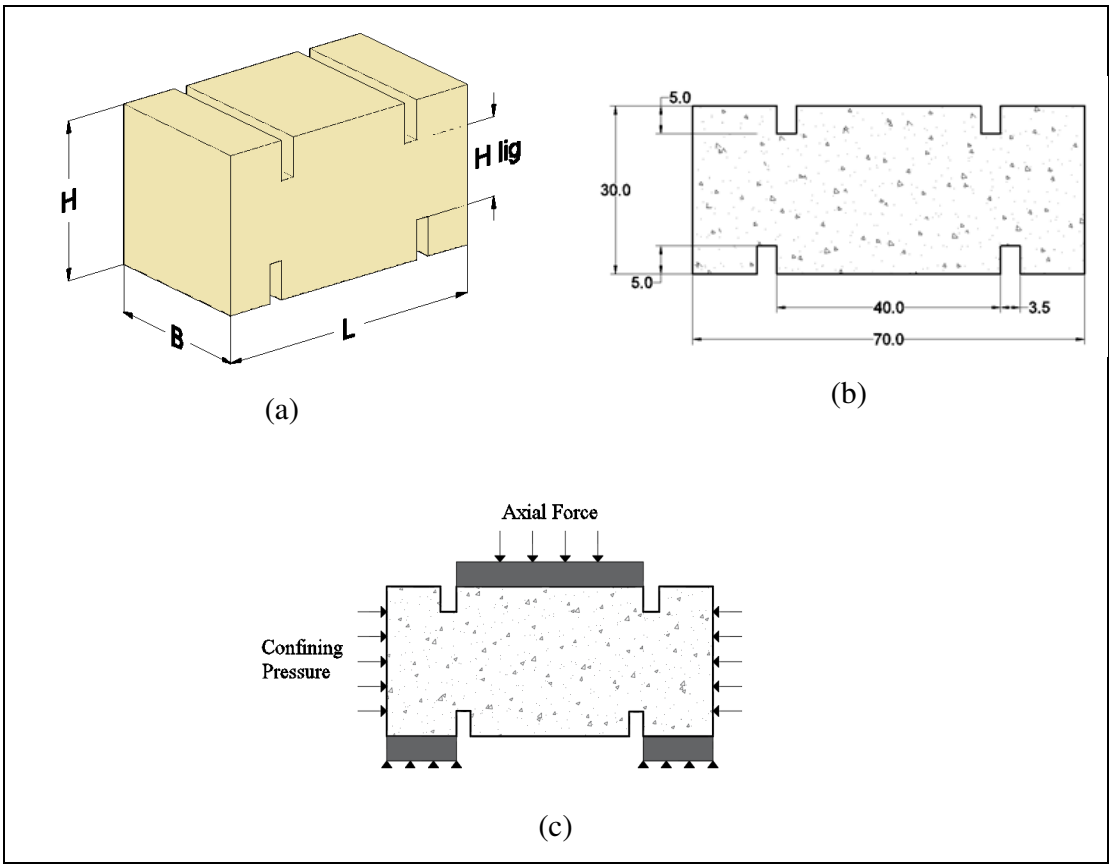

Figure 1 (a) 3D view of the specimen geometry. (b) Specimen dimensions. (c) Surfaces related to the application of the pre-stress (Confining Pressure) and the shear loading (Axial Force).

2.3. Sample Confinement

The sample confinement was fully described in [18]. It consists into deforming elastically a metallic cell and using the stored elastic energy to pre-stress the specimen. First, a compressive force (F_1) is applied to the cell along the Y direction (Figure 2). When the cell is enough deformed the concrete specimen is inserted inside. A certain number of steel sheets are used between the sample and the cell in order to adjust the level of needed confinement. Afterwards, the load F_1 is released. When the cell jaws get in contact with the sample, a compressive load is transferred to the specimen along the X direction up to the aimed lateral confinement stress. The deformation of the cell is measured during the loading and unloading by means of gages glued on the cell as shown in Figure 2.

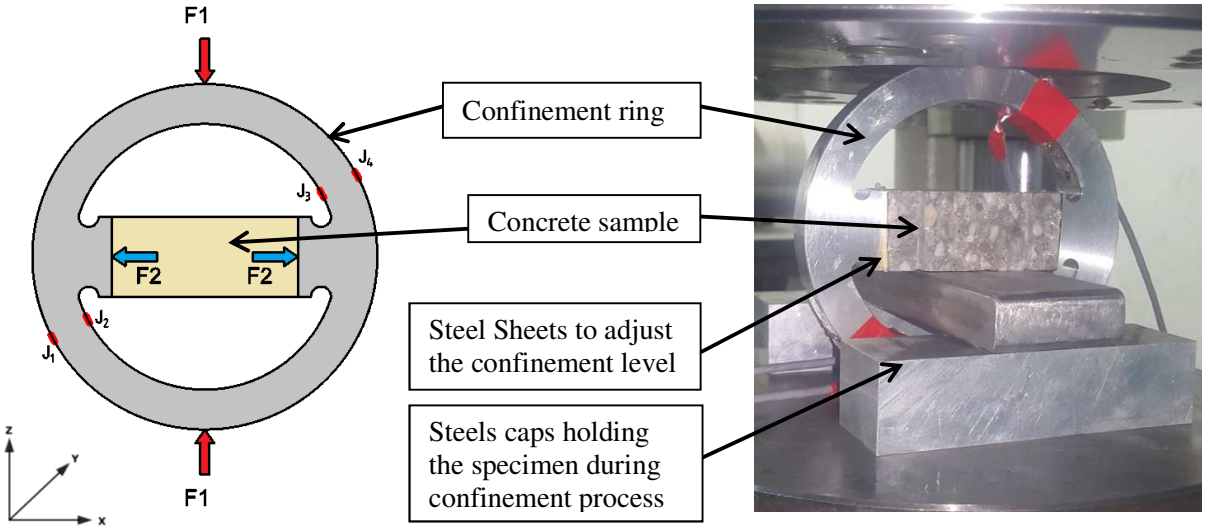

Figure 2 The location of the gages glued on the cell and the force applied to calibrate the gages

2.4. Cell calibration

Both aluminum and steel cells are instrumented with four strain gages glued on the internal and external surfaces of the cells as shown in Figure 2. The relation between the strain measured with each gage and the applied forces F_z and F_x (Figure 3) was established in [18]. This calibration allows us deducing the confinement pressure applied to the concrete sample from the gages signals. In a first step, a force F_z is applied (Figure 3(a)) and then the cell is rotated 90° and a force F_x is applied (Figure 3(b)).

$$F_z = \alpha^{-1}\varepsilon_i \qquad F_x = \beta^{-1}\varepsilon_i$$

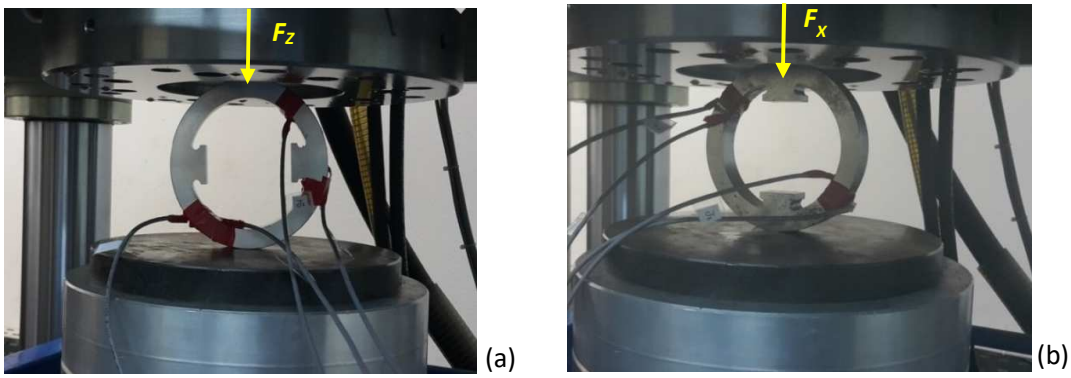

(a) (b)

Figure 3 The process of applying the forces F_x and F_z to calibrate the gages

For each case, the slope of the curve presenting the force as function of the measured strain at each gauge is calculated (*i* referring to the gage number from 1 to 4). The final relation for each gage is:

$$\varepsilon_i = \alpha_i F_x + \beta_i F_z \quad (1)$$

For each of the two rings (aluminum and steel), the coefficientsα andβ for each gauge are calculated and reported in Table 2.

Table 2 Coefficients of each gauge used to calculate the confinement pressure applied by means of an aluminum or steel cell

	Aluminum	Steel
α_1	-0.000138	-0.000045
α_2	0.000212	0.000071
α_3	0.000208	0.000021
α_4	-0.000057	-0.000047
β_1	0.000139	0.000047
β_2	-0.00014	-0.000048
β_3	-0.00014	-0.000014
β_4	0.00006	0.000051

The change of strain versus applied force F_z during a sample pre-stressing operation is plotted in the Figure 4. When the maximum force F_z is applied to the cell the specimen is inserted inside the cell jaws. In the unloading stage, when the specimen is get in contact with the cell, the strain-force slopes change as shown in Figure 4(b). At the final stage of unloading, the only load applied to the cell is the confinement force applied to the concrete sample F_x, which can be deduced from the measured strain of the gages ($\varepsilon_i = \beta_i F_x$ with $F_z = 0$). An example of the evolution of the forces applied during the pre-stressing stage of an aluminum cell is shown in Figure 4(b). In this example, a vertical load of about 15 kN is applied to the cell, the vertical load when the contact between the sample and the cell occurs is 13 kN, the force transferred to the concrete specimen is 11 kN (according to equation 1 and Table 2). The principle of samples pre-stressing is fully detailed in [18].

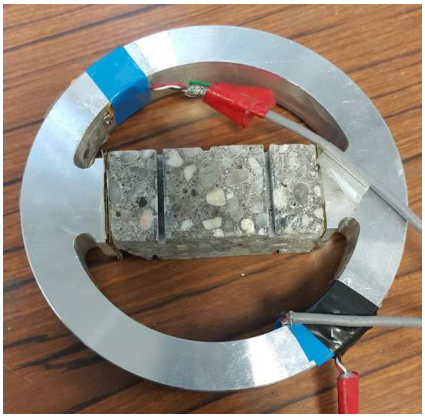

(a)

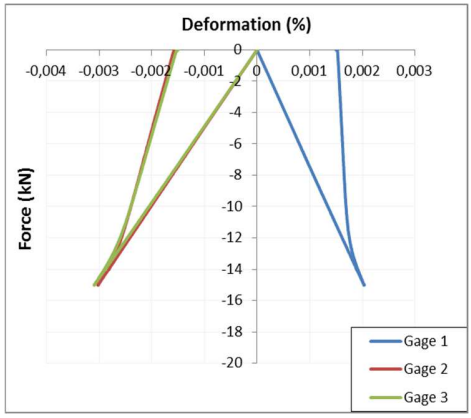

(b)

Figure 4 (a) A concrete specimen confined in-between the cell jaws (b) The evolution of the strain at each gage during confinement

3. Quasi-static shear tests

3.1 Experimental procedure

Quasi-static shear tests were conducted with a hydraulic press with a loading capacity of 100 tons. The tests were controlled in displacement with a driving speed sets to have a shear strain-rate of approximately $1e^{-4}$ s^{-1} in the elastic stage. A compression cylinder was used to apply the axial loading and intermediate rectangular supports were used between the specimen and the plate of the press. The test was instrumented with an LVDT sensor to measure the axial displacement of the central part. The schematic representation of quasi-static shear tests is shown in Figure 5.

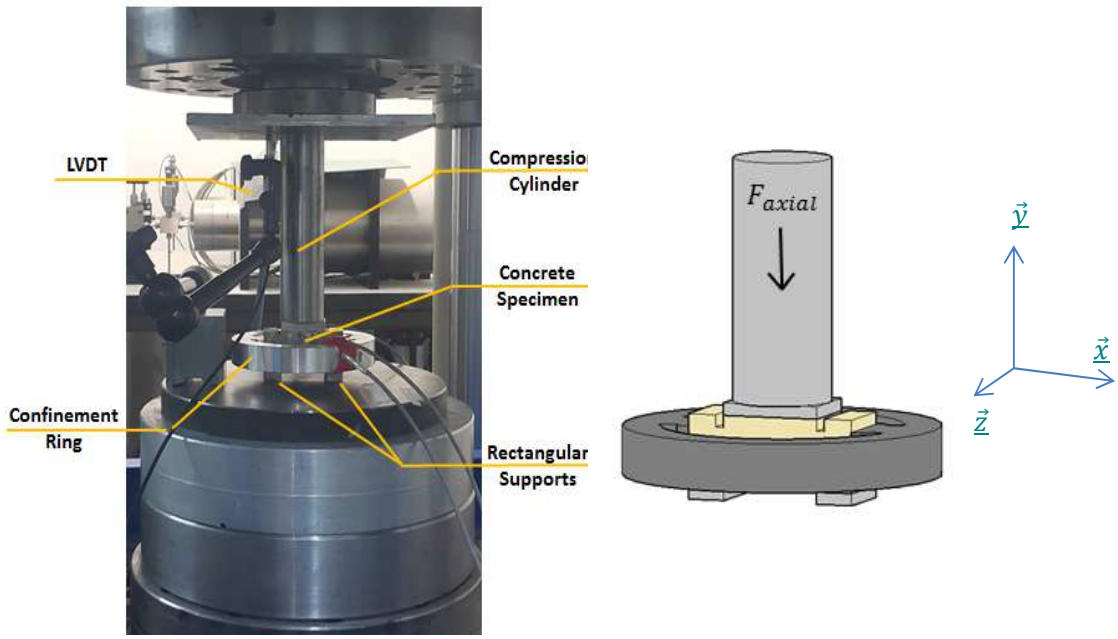

Figure 5 Schematic representation of the static Punch-through shear tests

3.2 Determination of radial and shear stresses

During the tests, the concrete sample exerts a force (F_x) on the metallic cell (cf. the frame in Figure 5) which deformation is measured by the strain gages. Using the processing technique described in section 2.3, one can deduce the change of mean radial pre-stress in the ligament during the test according to the formula:

$$\overline{\sigma_{xx}} = \frac{F_x}{S_{lig}/2} \quad (2a)$$

where S_{lig} corresponds to the shear surface of both ligaments.

$$S_{lig} = 2 \times B \times H_{lig} \quad (2b)$$

B being equal to 30 mm and H_{lig} equal to 20 mm (refer to Figure 1).

On the other hand, shear stresses are calculated by dividing the axial force measured by the press (F_y) by the shear surface.

$$\overline{\sigma_{shear}} = \frac{F_y}{S_{lig}} \quad (3)$$

3.3 Quasi-static tests results

3.3.1. Repeatability of tests

Several tests were performed twice to check the repeatability of results. For both tests, a good agreement between the two sets of results was noticed. Figure 6 shows two tests conducted on the same concrete with the same confining level. Same shear strength and mean confining stress were obtained for both tests in particular until the peak shear stress was reached.

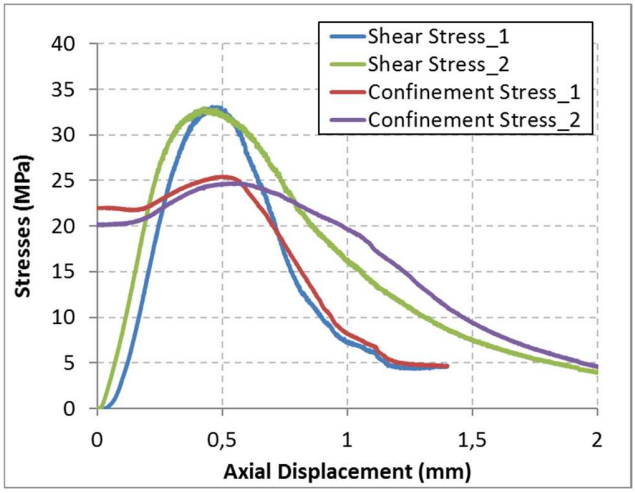

Figure 6 Results of two quasi-static shear tests performed on dry R30A7 concrete with a steel confining cell at the same confining level

A statistical study could be also conducted to asses for this repeatability. At the time of this investigation, it was not possible to do it in one batch because of the numerous tests with numerous conditions involved in this campaign. Then, the reader should be aware that this study is a first advanced step to understand the behaviour of concrete in these conditions. For researchers who would like to tackle this topic for a given composition of concrete, the latter would have to do numerous tests (at least six), for each level of pre-stress, to trustfully characterize the mechanical behaviour of the concrete to be studied, in order to ensure that the specimen manufacturing can not bias the results.

3.3.2. Influence of confinement pressure

Two types of cells were used, one made of a high-strength aluminum alloy and one made of steel. As the cell can be considered as a measurement device, the advantage of using an aluminum alloy cell is its smaller stiffness compared to the one made of steel. Indeed, for a

given applied load, higher deformations are obtained with the aluminum alloy cell and thus the signal to noise ratio is increased in comparison with the steel cell. On the other hand, the steel cell exhibits higher yield strength which allows sustaining higher force; therefore, higher confinement level can be reached. It is the reason why, the aluminum cell was used for small level of confinement and the steel cell was employed for the highest confinement values.

In order to study the influence of confinement on the concrete shear strength, experiments were carried out with both (aluminum alloy and steel) confinement cells. A comparison of shear experiments performed with dry concrete samples is presented in Figure 7.

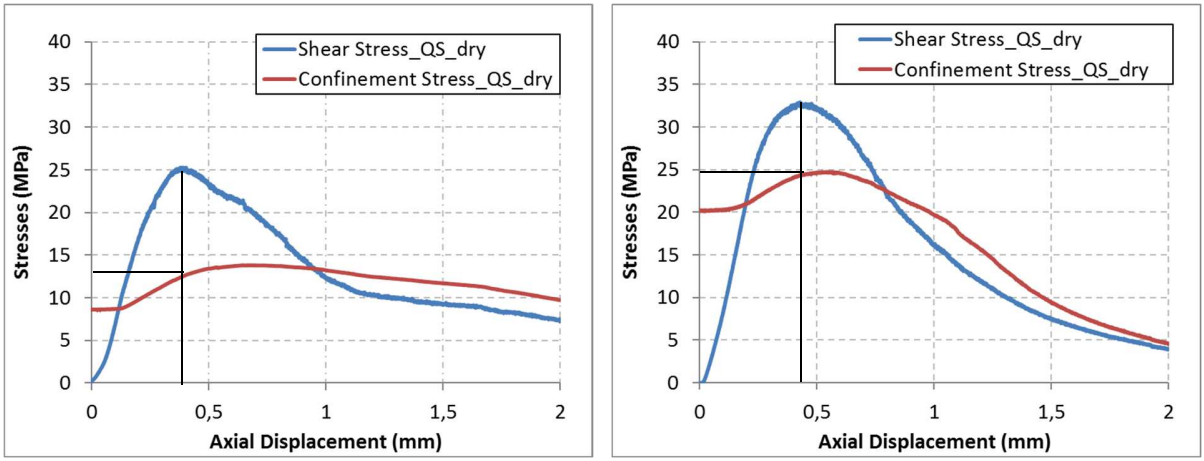

Figure 7 Results of quasi-static shear tests performed on dry R30A7concrete with (a) aluminum alloy and (b) steel confining cells

For the static shear test performed with the aluminum alloy cell (Figure 7a), the confinement stress is approximately equal to 9 MPa at the beginning of the test and increases up to 13 MPa when the shear stress reaches its peak, with a maximum value of 14 MPa after the peak. With the steel cell, the initial confinement is around 20 MPa and increases up to 25 MPa. For these different confining stresses, we can notice a difference in shear strength (defined at the maximum mean shear stress), i.e. 25 MPa for the aluminum alloy cell and 33 MPa for the steel one. Therefore, it is observed that by changing the stiffness of the cell the confinement level in the concrete sample is changed resulting in different shear strength. Finally, it is concluded that concrete is pressure sensitive under shear loading as observed in previous work [13; 24].

3.3.3. Influence of moisture content

To study the influence of moisture content, experiments were conducted with dry and wet specimens. The saturated specimens were kept in water until few minutes before testing. The

212 ‘‘dried’’ specimens were oven-dried at 60°C during several weeks until a constant weight has
213 been achieved. The results of two quasi-static tests performed with an aluminum alloy cell are
214 reported on Figure 8.
215

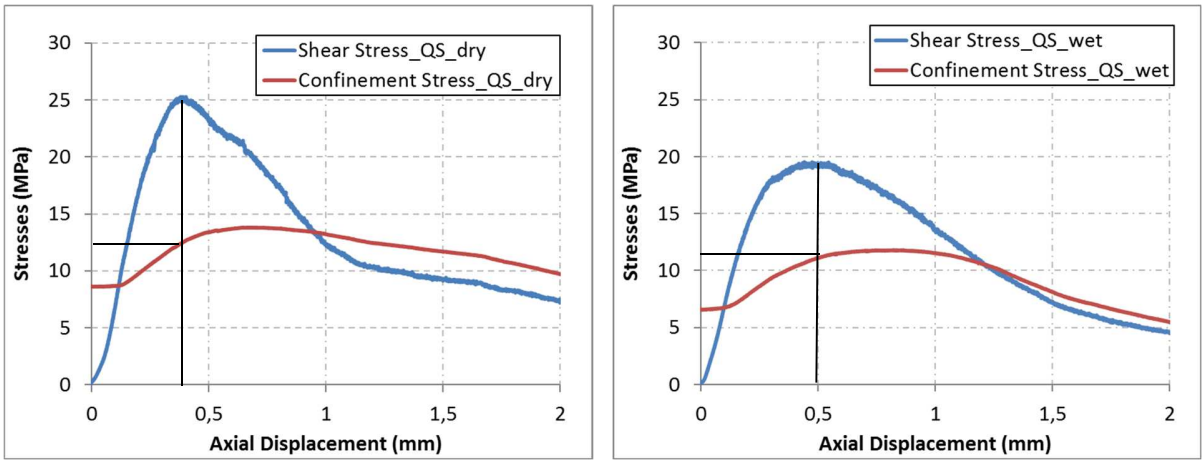

216
217 **Figure 8 Results of quasi-static shear tests performed with an aluminum cell on (a) dry and (b) wet R30A7**
218 **concrete specimens.**

219 For approximately the same confinement level, the maximum shear stress reached in wet
220 specimen was 19 MPa while on the other hand, the dry sample exhibited higher shear strength
221 of about 25 MPa. This result is consistent with the one reported by [13] with (non-pre-stressed)
222 “passive confinement” cell.

223 **3.3.4. Post-mortem observation**

224 Videos and pictures were taken during the static testing in order to follow the development of
225 visible surface cracks. The propagation of crack was analyzed for the test called 'shearstat06' at
226 different stages of loading (Figure 9).
227 It was noticed that a main planar shear fracture connected to the two notches develop from each
228 side of the specimen; this fracture corresponds to the expected Mode II fracture and seems to
229 initiate at the peak of loading (Figure 9 (b)) as no fracture is visible on the sample surface prior
230 the shear stress peak (Figure 9 (a)).

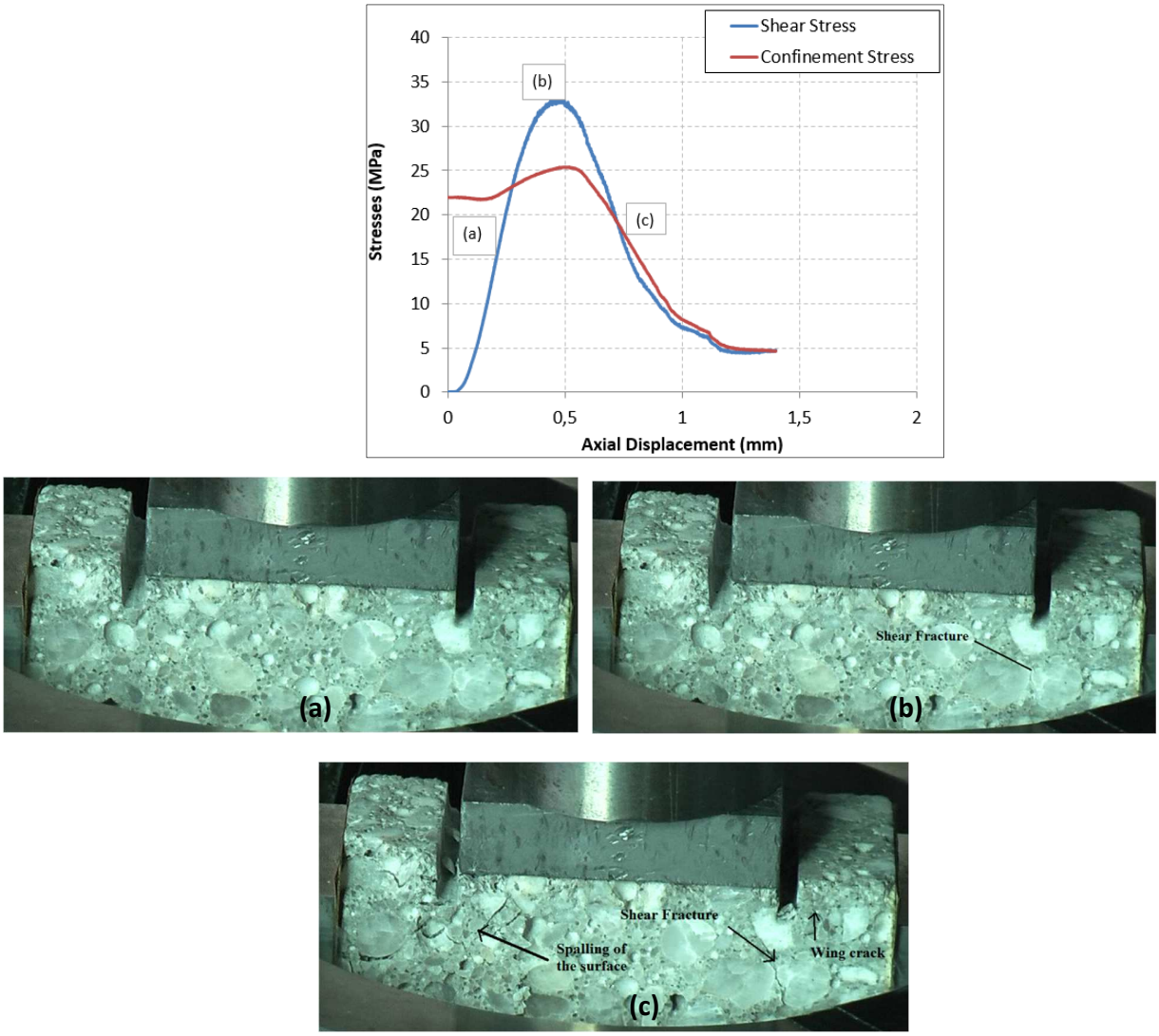

231

232 **Figure 9. Fracturing on the surface of a dry concrete sample at different stages of static loading.**

233 In parallel to the mode II fracture, wing cracks are initiated (Figure 9(c)) at the tip of the
234 sample upper notch. These cracks were not observed before the peak and seem to appear after
235 the peak. Since only the surface of the sample is visualized, it is difficult to know if these
236 cracks were initiated before or after the peak in the core of concrete. It was stated by Watkins
237 [5] and Backers [25] that these cracks should initiate before the peak but stop and should not
238 influence the principle mode II fracturing.

239

240 ## 4. Dynamic shear tests

4.1. Split Hopkinson Pressure Bar Technique

The dynamic loading is applied to the specimen through a Split Hopkinson bar apparatus. It is composed of a striker bar, 480 mm in length and 45 mm in diameter, made of high strength aluminum alloy striking an incident bar of 1500 mm in length and 45 mm in diameter made of the same alloy. In addition, two output bars, 1200 mm in length and 20 mm in diameter, made of steel are used. The three cylindrical Hopkinson bars are instrumented with strain-gages. A pulse shaper technique is used in order to increase the rising time and to reach static force equilibrium (equality of input and output forces) in the specimen at the shear stress peak. To do so, a thin disk of lead is attached to the impacted end of the incident bar to generate an incident wave characterized by a longer rising time. The experimental setup is schematically shown in Figure 10.

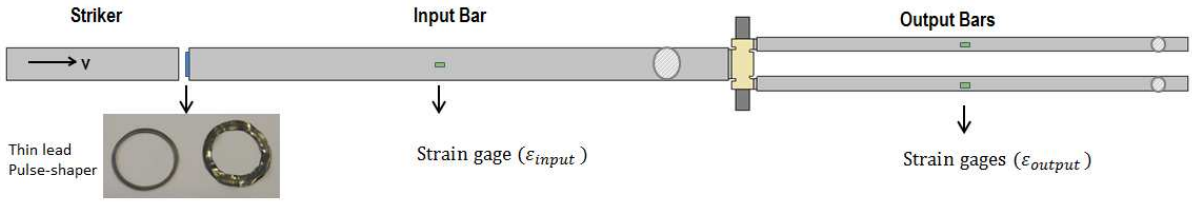

Figure 10 Schematic representation of the SPHB system for dynamic Punch-through shear tests

The compressive incident wave travels through the input bar to the specimen interface where it is divided into a reflected wave propagating back into the input bar and a transmitted wave passing through the sample and traveling through the output bars. Based on the axial strains measured in the bars and according to the one dimensional wave theory, forces and particles velocities at each bar/specimen interface can be calculated [26].

4.2 Processing technique

The forces and particles velocities at the specimen faces are calculated by shifting the waves to the same points assuming that no wave dispersion occurs in the slender elastic bars. Considering $\varepsilon_{incident}$, $\varepsilon_{reflected}$ and $\varepsilon_{transmitted}$ the shifted incident, reflected and transmitted wave respectively, the forces and velocities at the contact surfaces can be calculated as follows:

$$\begin{cases} F_{input} = -S_{input}\, E_{bar}\, (\varepsilon_{incident} - \varepsilon_{reflected}) \\ F_{output} = -S_{output}\, E_{bar}\, \varepsilon_{transmitted} \\ V_{input} = -C_{bar}\, (\varepsilon_{incident} - \varepsilon_{reflected}) \\ V_{output} = -C_{bar}\, \varepsilon_{transmitted} \end{cases}, \quad (4)$$

where F_{input} and F_{output} are the input and output forces, V_{input} and V_{output} are the particle velocities at the incident and transmitted bars ends, S_{input} and S_{output} are the cross section areas of the incident and output bars, E_{bar} is the Young's modulus of the bar and C_{bar} the elastic wave speed of the bar.

The axial displacement is then deduced by integrating the axial velocity obtained as follows:

$$V_{axial} = V_{input} - V_{output} \quad (5)$$

The mean axial force is deduced by averaging the input and output forces as follows:

$$F_{axial} = \frac{F_{input} + F_{output}}{2} \quad (6)$$

This processing technique was applied to a series of dynamic experiments performed on wet specimens. Experimental results are presented hereafter.

4.3 Dynamic tests results

The experimental setup used for dynamic tests is presented in Figure 11.

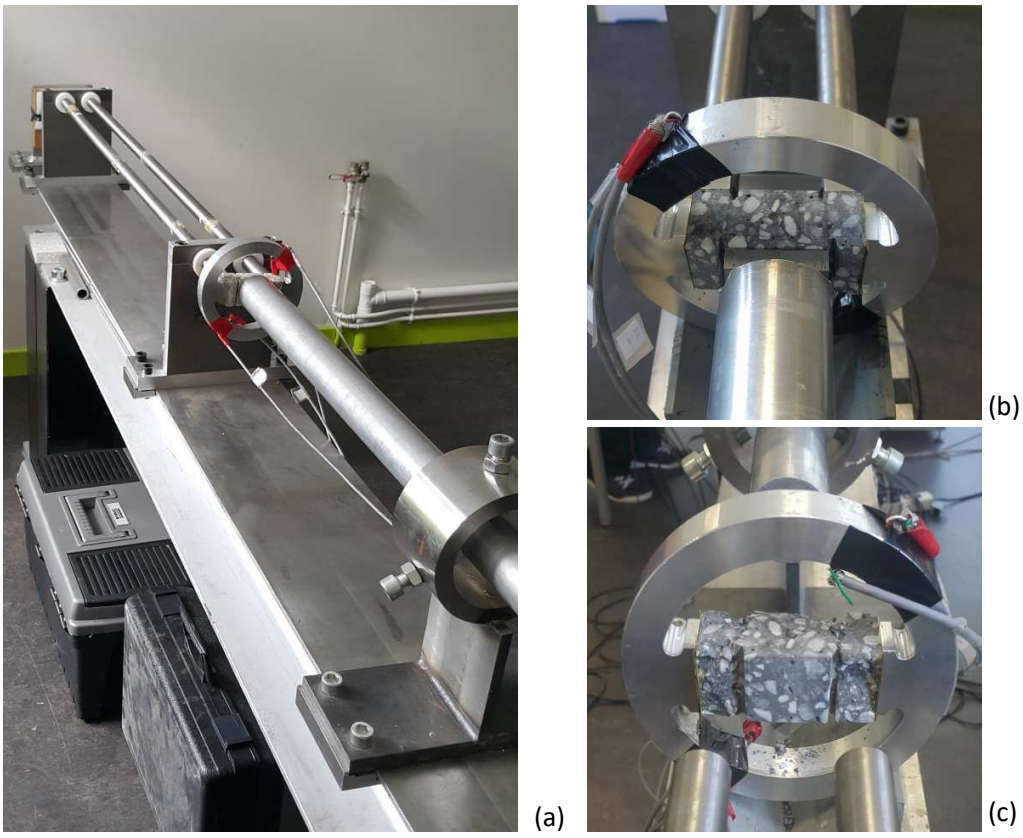

Figure 11 Experimental device used for dynamic tests (a) General view of the setup (b) zoom on a concrete sample with the confinement cell before testing (c) Concrete sample after shearing

The input bar was instrumented with strain gages glued at different locations on the input bar: one at the quarter length and the other one at the mid length of the input bar whereas a strain gage was glued in the middle of each output bar. Typical strain gage signals measured in dynamic test are shown in Figure 12(a). The shifted forces deduced at both ends of the sample are shown in Figure 12(b).

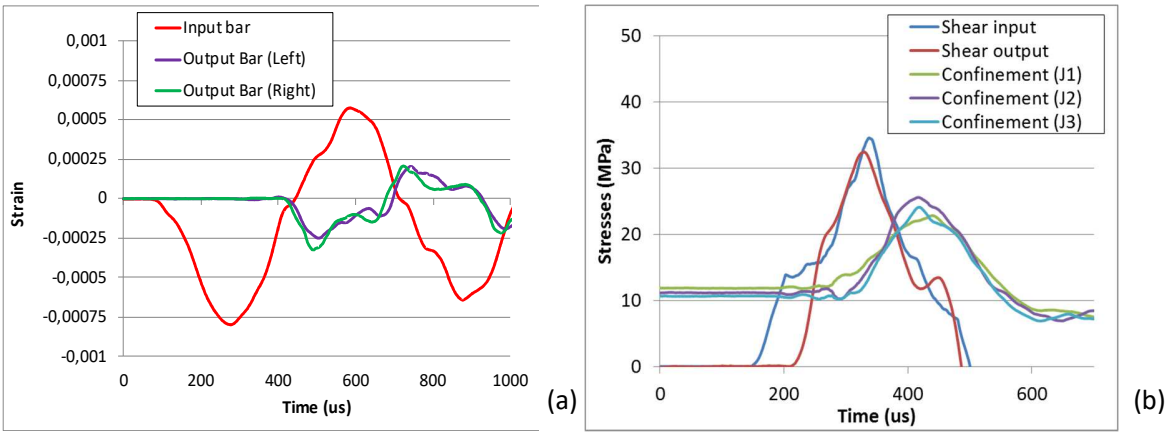

Figure 12 Results for a typical dynamic test (a) Signals recorded by strain gages (b) Forces deduced at the bar/sample interfaces.

First, it is observed that the two signals measured on each output bars (left and right) are very similar. This result also observed in the other dynamic tests tends to demonstrate that the same shear force is generated in both sample ligaments and the test is well symmetric. The total output force was then obtained by adding the two forces extracted from these two signals.

The profiles of mean shear strength calculated from the input and output forces are plotted as function of time in Figure 12(b). It can be seen that the curves are very close above 16 MPa, which means that the force equilibrium condition inside the sample is well insured at the peak of the shear stress. Finally, the mean shear stress in the ligament is obtained by averaging the input and output forces divided by the section of the ligament:

$$\sigma_{shear} = \frac{F_{input} + F_{output}}{2\, S_{lig}} \tag{10}$$

The strain rate of dynamic tests is estimated from the time evolution in the elastic stage by measuring the slope of the shear stress versus time:

$$\dot{\gamma}_{shear} = \frac{\dot{\sigma}_{shear}}{G}, \tag{11}$$

where G is the shear modulus ($G = E/(2+2\nu)$). A typical dynamic shear deformation curve in the dynamic PTS sample is shown in Figure 13. The output stress divided by the concrete shear modulus is drawn as function of time and the slope of this curve is defined as the loading rate. This method was used to determine the loading rate for each dynamic punching-through shear

test. Projectile impact velocity was similar for all the tests (around 9 m/s) resulting in loading rates ranging from 27 s^{-1} to 40 s^{-1}.

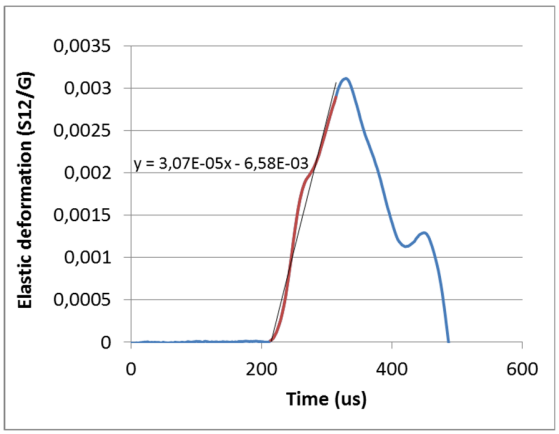

Figure 13 Typical elastic shear deformation curve for determining the strain-rate of dynamic tests

4.3.1 Influence of confinement

As in quasi-static tests, both confinement cells (aluminum alloy and steel cells) were employed to investigate the effect of confinement level on the shear response of concrete. A comparison of shear tests conducted on dry samples is presented in Figure 14. It is observed that when the confinement level increases, an increase of the shear strength of concrete is noted. For of confinement stress of 15 MPa at the peak of shear stress, concrete exhibits shear strength of 30 MPa whereas the shear strength reaches a much higher value (45 MPa) at higher confinement level (27 MPa).

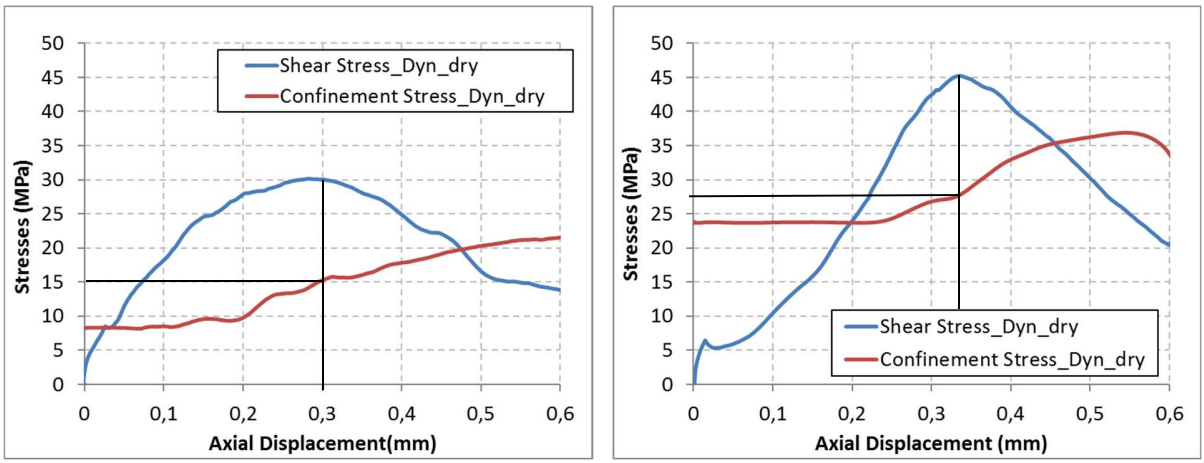

Figure 14 Results of dynamic shear tests performed on dry specimens with (a) aluminum and (b) steel confining cells

4.3.2 Influence of moisture content

A series of experiments was conducted considering different moisture content. Dynamic test results obtained with dry and water saturated specimens with an aluminum alloy confining cell are reported on Figure 15. Whereas for the confinement stress is almost identical with wet and dry specimens the shear strength of wet samples (28 MPa) is much lower than the one of dry ones (37 MPa).

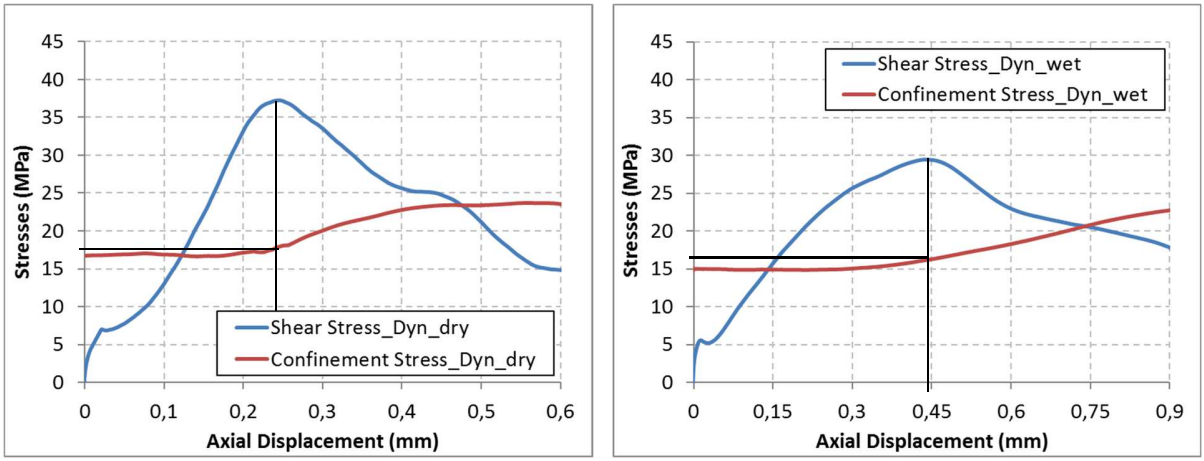

Figure 15 Results of dynamic shear tests performed with an aluminum cell on (a) dry and (b) wet specimens

4.3.3. Post-mortem observation

Figure 16 Crack pattern for a concrete sample subjected to dynamic shearing

Similar cracking patterns were observed in both quasi-static and dynamic experiments. The main fracture plane is clearly noticeable in the pictures of Figure 16; it propagates almost perfectly straight and it is connected to both top and bottom notches. X-ray micro tomography technique was used to investigate the micro-cracks inside the tested concrete sample.

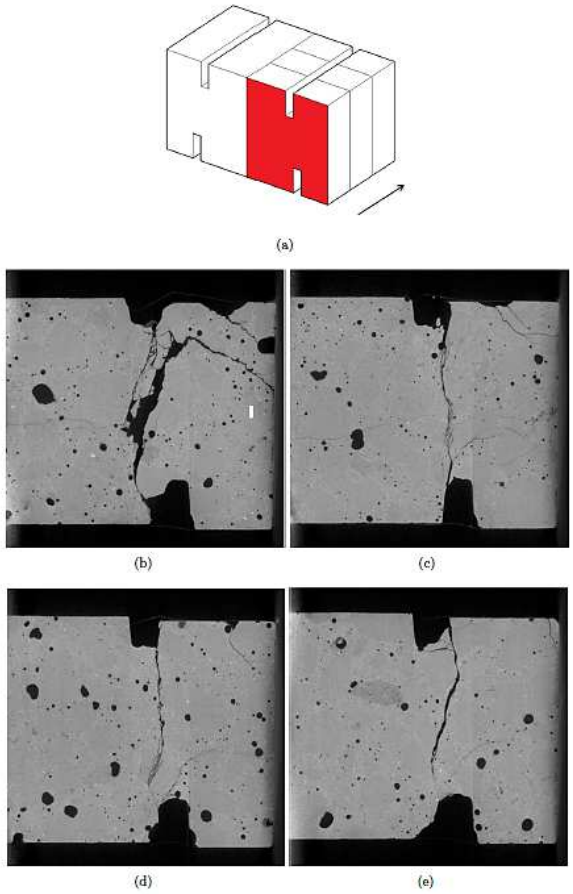

Figure 17 CT scans on a tested concrete specimen at different depths (b) 0mm (c) 10mm (d) 20mm and (e) 30mm.

The multi-scale X-ray tomograph manufactured by RX-solutions Company was used at 150 kV and 140 µA. The exposure time is 0.5 s. An average of 6 images is used to obtain 1440 radiographies leading to a scanning time equal to one hour. The CT images have a resolution of 29 µm that corresponds to the maximum possible zooming to ensure that half the specimen is scanned. This resolution is sufficient to analyze the fracture pattern of the fractured sample. Figure 17 represents the CT images of four cross-sections spaced of 10 mm and located at 0, 10, 20 and 30 mm through the sample depth. The vertical shear surface (mode II) inside the ligament is clearly visible at different locations inside the concrete sample which means that this vertical fracture occurs throughout the volume.

5. Discussion: influence of strain-rate and confinement level

A series of tests have been performed on concrete considering two types of moisture content, different levels of confinement and both static and dynamic conditions. A summary of all the obtained results is presented hereafter.

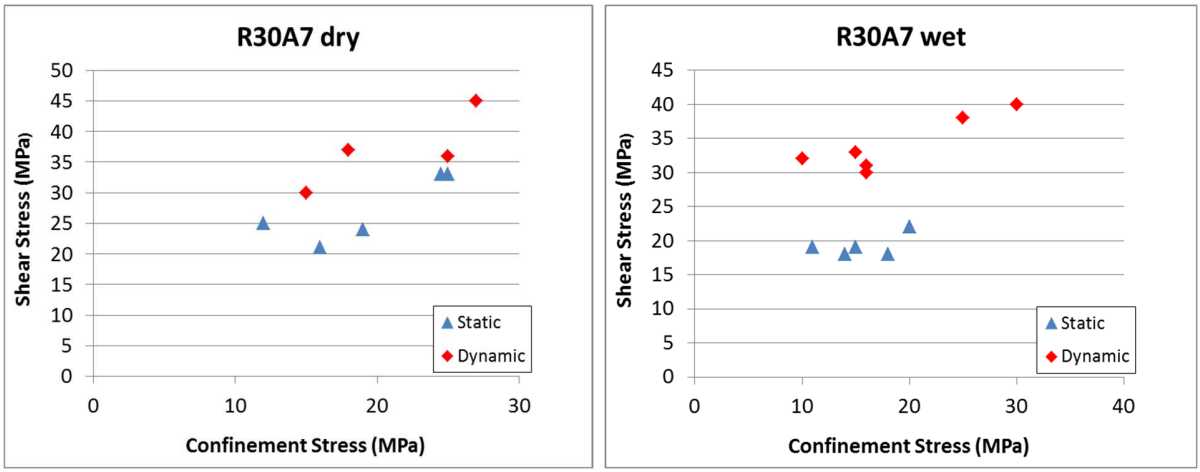

(a) (b)

Figure 18 Shear stress in function of the confinement stress calculated in the ligament of a concrete sample in quasi-static and dynamic conditions (a) dry (b) wet concrete.

Figure 18 illustrates the shear strength of concrete as function of the confinement stress (at the peak of shear stress) for both sets of tests (static and dynamic) and for both batches of concrete samples (dry and saturated R30A7 concrete).

On the one hand, for both loading-rate conditions (static and dynamic), it is clear that the shear strength increases with the confining level. This trend is easily observed with dry samples and with wet samples tested in dynamic condition. For instance, given a confinement stress of 10 MPa, the shear stress obtained in wet concrete is around 32 MPa whereas it reaches about 40 MPa for a confinement of 30 MPa. Unfortunately, it was difficult to reach higher confinement level for wet R30A7 concrete, because concrete sample could be damaged due to compression stresses before applying the shear loading. The same trend was noticed for dry R30A7. In static conditions, the maximum shear stress reaches 25 MPa for a confinement level of 12 MPa whereas the shear strength increases up to 33 MPa at 25 MPa of confinement stress. In dynamic conditions, the increase of shear strength in dry concrete is even more spectacular from 30 MPa up to 45 MPa when the confinement stress increases from 15 MPa to 27MPa.

On the other hand, for a given level of confinement stress, higher shear strength is noted in dynamic testing conditions than in static ones. This result is clear for wet R30A7 concrete for

371 which the shear strength is around 20 MPa in static tests and around 35 MPa in dynamic ones
372 given a confinement of 17 MPa. (Figure 18(b)). For dry R30A7 concrete, if ones consider a
373 confinement level of 16 MPa for instance, the shear strength in quasi-static conditions is around
374 21 MPa while it reaches 30 MPa in dynamic conditions (Figure 18(a)).
375 The influence of confinement and strain rate on concrete was also displayed in a different way;
376 the shear stress was plotted as function of the strain rate for both types of concrete (Figure 19).
377 The size of the points plotted for each test depends on the level of confinement at the peak of
378 the shear stress.
379

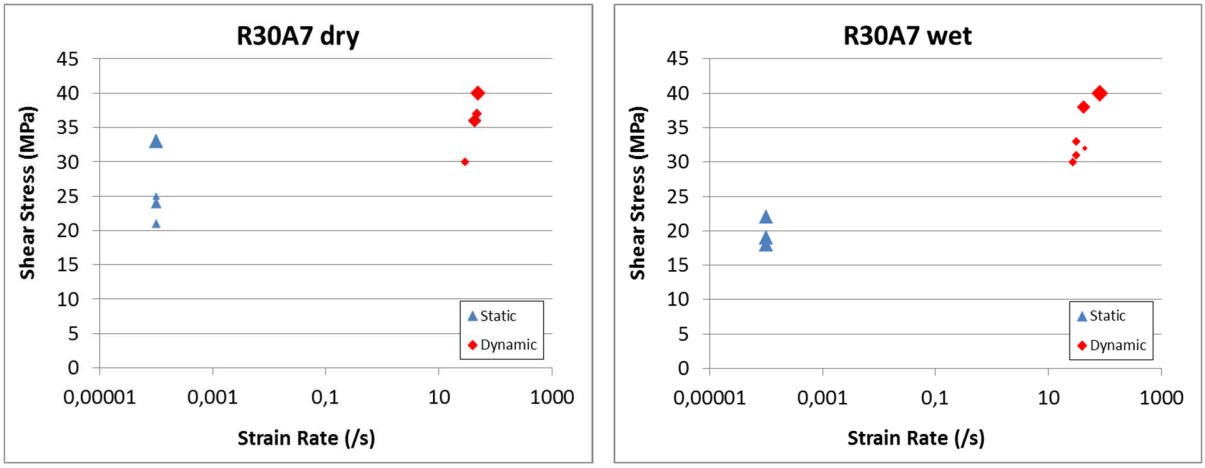

(a) (b)

380
381 **Figure 19 Shear stress in function of the strain rate in quasi static and dynamic conditions (a) dry concrete**
382 **(b) wet concrete.**

383 Although a small scatter in the test results is observed, these figures clearly indicate that the
384 shear strength of concrete depends on the confining pressure and on the applied loading-rate.
385

386 ## 6. Conclusion

387 The security of concrete structures used in many applications such as nuclear containments,
388 bunkers or dams is of considerable concern since these structures can be exposed to various
389 extreme loadings during which different compressive, tensile and shear failure modes might be
390 observed. Various experimental methods have been used to explore the behavior of concrete
391 under different types of loading over a wide range of strain rates. It was shown in the literature
392 that concrete exhibits an increase of strength under confinement (triaxial and quasi-oedometric

compression tests) and dynamic tensile loadings (spalling tests). However, in contrast to tensile behavior, the shear behavior of concrete under compression and dynamic loadings has not been carefully studied at constant confinement level.

The aim of the present work is to investigate the quasi-static and dynamic shear behavior of concrete under confined conditions. In previous experiments, concrete samples were either subjected to a small level of confinement [7] or a high level of confinement with a passive metallic cell [14]. In the last method, a strong change of confinement level occurs during the tests and constitutes a major drawback of this technique. In this work, a method has been developed to apply a confinement to samples before testing them under shear. It consists in inserting a concrete specimen into a pre-stressed metallic cell. When the loading is released, confining stresses are transferred to the ligament of the concrete sample. Then, a vertical displacement is applied to the central part of the sample to produce shear deformation in the ligament. Two types of metallic cell were used (aluminum and steel) in order to study the influence of confinement. Finally, higher shear strength was reported with higher confinement which confirms the pressure sensitivity of concrete. Dynamic tests performed with the Split Hopkinson Bar technique were performed to analyze the effect of strain-rate on the confined shear behavior of concrete. It was observed that at the same level of confinement, concrete samples subjected to dynamic loadings exhibits higher shear strength than the ones subjected to static loadings. Moreover, considering dried and saturated samples it was noted that dry samples exhibit higher shear strength than saturated ones. An integration of the reported experimental data into a constitutive or numerical model describing the shear behavior of concrete as function of the applied strain-rate and confinement constitutes a naturel prospect of the current work.

Acknowledgements

This research has been performed with the financial support of the CEA-Gramat Research Center (France) and the doctoral school IMEP2 of Grenoble Alpes University. This support is gratefully acknowledged.

This work has been supported by the LabEx Tec 21 (Investissements d'Avenir, grant agreement no. ANR-11-LABX- 0030).

References

[1] Zukas, J. 1992. *Penetration and perforation of solids*. Impact dyn. Krieger Publishing Company.

[2] Forquin, P., Arias, A., Zaera, R. 2008. "Role of porosity in controlling the mechanical and impact behaviours of cement-based materials." *International Journal of Impact Engineering* 35(3): 133–146.

[3] Ingraffea, A.R., Panthaki, N.J. 1985. "Analysis of shear fracture tests of concrete beams." In *Japan Seminar on Finite element Analysis of reinforced concrete structures, Tokio*, p. 71–91.

[4] Bazant, Z.P., Pfeiffer, P.A. 1986. "Shear fracture tests of concrete." *Materials and Structures* 19(110): 111–121.

[5] Watkins, J. 1983. "Fracture toughness test for soil-cement samples in mode II." *International Journal of Fracture* 23: 135–138.

[6] Luong, M.P. 1992. "Fracture testing of concrete and rock materials." *Nuclear engineering and design* 133: 83–95.

[7] Montenegro, O.I., Sfer, D., Carol, I. 2007. "Characterization of concrete in mixed mode fracture under confined conditions." In *ICEM13 conference, Alexandroupolis, Greece*.

[8] Backers, T., Dresen, G., Rybacki, E., Stephansson, O. 2004. "New data on mode II fracture toughness of rock from the punch-through shear test." *International Journal of Rock Mechanics and Mining Sciences* 41(3): 1–6.

[9] Montenegro, O.I., Sfer, D., López, C.M., Carol, I. 2013. "Experimenal tests and numerical modeling to identify the asymptotic shear-compression mode IIA of concrete fracture." In *VIII International Conference on Fracture Mechanics of Concrete and Concrete Structures FraMCoS-8*.

448 [10] Backers, T., Stephansson, O., 2012. "ISRM suggested method for the determination of
449 Mode II fracture toughness." *Rock Mech. Rock Eng.* 45: 1011-1022.

450 [11] Li, L.R., Deng, J.H., Liu, J.F., Zheng, J., Chen, T., Deng, C.F., 2017. "A new
451 understanding of punch-through shear testing. " *Géotechnique Letters* 7(2), 1-7.

452 [12] Xu, Y., Yao, W., Xia, K., Ghaffari, H.O. 2019. "Experimental Study of the Dynamic Shear
453 Response of Rocks Using a Modified Punch Shear Method." Rock Mech. Rock Eng. 52:
454 2523-2534.

455 [13] Forquin, P. 2011a. "Influence of free water and strain-rate on the shear behaviour of
456 concrete." eds. Ezio Cadoni and Marco Di Prisco. *Applied mechanics and materials* 82:
457 148–153.

458 [14] Forquin, P., Sallier, L. 2013. "A testing technique to characterise the shear behaviour of
459 concrete at high strain-rates." In *Dynamic behavior of Materials, Volume1*, eds. Vijay
460 Chalivendra, Bo Song, and Daniel Casem. Springer New York, p. 531–536.

461 [15] Lukić, B., Forquin, P. 2015. "Experimental characterization of the punch through shear
462 strength of an ultra-high performance concrete." *International Journal of Impact*
463 *Engineering* 91: 34–45.

464 [16] Yao, W., Xu, Y., Yu, C., Xia, K. 2017. "A dynamic punch-through shear method for
465 determining dynamic Mode II fracture toughness of rocks." *Engineering Fracture*
466 *Mechanics* 176: 161–177.

467 [17] Xu, Z.-J., Ding, X., Zhang, W., Huang, F. 2017. "A novel method in dynamic shear testing
468 of bulk materials using the traditional SHPB technique." *International Journal of Impact*
469 *Engineering* 101: 90–104.

470 [18] Forquin, P., Abdul-Rahman, R., Saletti, D. 2020. Submitted for publication. A novel
471 experimental method to characterize the shear strength of concrete based on pre-stressed
472 samples.

473 [19] Gabet, T., Malécot, Y., Daudeville, L. 2008. “Triaxial behaviour of concrete under high
474 stresses: Influence of the loading path on compaction and limit states.” *Cement and*
475 *Concrete Research* 38(3): 403–412. October 16, 2014.

476 [20] Vu, X.-H., Malecot, Y., Daudeville, L., Buzaud, E. 2009. “Experimental analysis of
477 concrete behavior under high confinement: Effect of the saturation ratio.” *International*
478 *Journal of Solids and Structures* 46(5): 1105–1120.

479 [21] Zingg, L., Briffaut, M., Baroth, J., Malecot, Y. 2016. “Influence of cement matrix porosity
480 on the triaxial behaviour of concrete.” *Cement and Concrete Research* 80: 52–59.

481 [22] Piotrowska, E., Forquin, P., Malecot, Y., 2016. “Experimental study of static and dynamic
482 behavior of concrete under high confinement: effect of coarse aggregates strength.” *Mech.*
483 *Mat.* 92: 164–174.

484 [23] Regal, X., Hanus, J.-L., 2017. “Experimental Study of the Dynamic Flexural Strength of
485 Concrete. Experimental Mechanics.” 57: 427-442.

486 [24] Forquin, P. 2011b. “Influence of strain-rate and confining pressure on the shear strength of
487 concrete.” In *Dynamic Behavior of Materials, Volume 1*, Springer New York, p. 29–35.

488 [25] Backers, T., Stephansson, O., Rybacki, E. 2002. “Rock fracture toughness testing in Mode
489 II - punch-through shear test.” *International Journal of Rock Mechanics and Mining*
490 *Sciences* 39: 755–769.

491 [26] Kolsky, H. 1949. “An Investigation of the Mechanical Properties of Materials at very High
492 Rates of Loading.” *Proceedings of the Physical society. Section B* 62(11): 676–700.

493